In Vivo Studies of Dialkynoyl Analogues of DOTAP Demonstrate Improved Gene Transfer Efficiency of Cationic Liposomes in Mouse Lung

Steven Fletcher,[†,‡] Ayesha Ahmad,[†] Eric Perouzel,[§] Andrew Heron,[||] Andrew D. Miller,*[,†,§] and Michael R. Jorgensen*[,§]

Imperial College Genetic Therapies Centre, Department of Chemistry, Flowers Building, Armstrong Road, Imperial College London, London, SW7 2AZ, UK, and IC-Vec Ltd, 13 Prince's Gardens, London, SW7 1NA, UK

Received July 27, 2005

A novel set of dialkynoyl analogues of the cationic, gene delivery lipid DOTAP (**1**) was synthesized. Structure−activity studies demonstrate that replacement of the cis-double bonds of DOTAP with triple bonds in varying positions alters both the physical properties of the resultant cationic liposome−DNA complexes and their biological functionalities, both in vitro and in vivo. Particularly, in vivo studies demonstrate that pDNA transfection of mouse lung endothelial cells with lead analogue DS(14-yne)TAP (**4**):cholesterol lipoplexes exhibits double the transfection level with less associated toxicity relative to the well-established DOTAP:cholesterol system. In fact, **4**:cholesterol delivers up to 3 times the dose of pDNA in mice than can be tolerated by DOTAP, leading to nearly 3 times greater marker-gene expression. X-ray diffraction studies suggest that lipoplexes containing analogue **4** display increased stability at physiological temperatures. Our results thus suggest that analogue **4** is a potentially strong candidate for the gene therapy of lung tumors.

Introduction

The delivery of plasmid DNA (pDNA) to cells in order to effect transgene expression, and the delivery of antisense oligonucleotides (ONs) and small interference RNAs (siRNAs) to achieve gene silencing have fast become popular probes of gene and protein function. In particular, the intracellular delivery of nucleic acids may facilitate the treatment or cure of genetically-based diseases, both inherited, such as cystic fibrosis and Parkinson's, and acquired, such as cancer and HIV/AIDS. To this end, liposome/micelle-based gene delivery has emerged as a prevalent method for non-viral gene therapy applications.[1−4] However, despite several inherent advantages over viral vectors, cationic liposome/micelle−DNA complex (lipoplex, LD) systems have, to date, met with limited success in vivo.

Simple cationic liposomes (comprised of a cationic lipid and usually a neutral, helper lipid such as cholesterol) are used to condense DNA into cationic lipoplexes that are able to afford the DNA limited protection from plasma nucleases.[5,6] The positive charge of the lipoplex is useful for binding to negatively charged cell surfaces in vitro, and thus these lipoplexes are found to be efficient transfection agents.[7] However, the positive charge has its disadvantages in vivo, where it results in the rapid formation of aggregates with anionic plasma proteins, thereby labeling the lipoplexes for clearance by the liver.[6,8,9] Such lipoplexes are initially found mostly in the lung shortly after i.v. injection due to the first-pass effect where the aggregates are captured by the primary capillary bed encountered.[8−14] Consequently, with such systems, the highest level of gene expression is observed there due to uptake of some of the lipoplex particles and/or aggregates by lung endothelial cells. Most of the residual lipoplexes or aggregates are then redistributed to the liver, where Kupffer cells are responsible for uptake.[11−15] Liver uptake is usually associated with DNA degradation and poor expression levels.

While the in vivo gene therapy of synthetic vectors lags behind the corresponding success of their viral counterparts, the cationic lipid (cytofectin) *N*-[1-(2,3-dioleoyloxy)propyl]-*N*,*N*,*N*-trimethylammonium methyl sulfate (DOTAP, **1**) has proven moderately successful for the in vivo gene therapy of pulmonary diseases in animal models.[13,16,17] Indeed, it is the most widely used cationic lipid, efficient both in vitro and in vivo. For instance, DOTAP:cholesterol lipoplexes have been shown to deliver tumor-suppressor genes to primary and disseminated lung tumors in vivo, resulting in the suppression of tumor growth.[18−20] In fact, phase I clinical trials for the systemic treatment of lung cancer tumor suppressor genes have recently been initiated.[18] One caveat to the use of such DOTAP lipoplexes is that they induce inflammatory responses in a dose-dependent fashion, and doses above 50 μg of pDNA are not tolerated in mice.[13,16,18,21−25] High transgene expression in mouse lung has also been correlated with hepatoxicity, although this is probably related to nonmethylated CpG sequences in the pDNA.[13,22,23] These problems have served to limit the therapeutic potential of DOTAP lipoplexes.

As a result of these aforementioned issues, many new lipids with various chemical and physical properties have been synthesized to overcome these biological barriers that impede the path of cationic lipoplexes.[1,2] For example, several groups have focused on the modification of the cationic headgroup[26−28] or on imparting particular biological instabilities, such as sensitivity to pH.[29,30] In contrast, there has been relatively little attention given to the hydrophobic lipid tails that dictate how fluid liposomal bilayers will be, which, in turn, will influence transfection potency by conferring instability when in contact with anionic cellular membranes.[31,32] The reason for this neglect may arise from the observation that fully saturated lipid tails, relative to the common oleate (C18:Δ^9) tails, typically lead to a substantial reduction in transfection in vitro.[33]

In our present strategy, we have attempted to improve the in vivo characteristics and toxicity profile of DOTAP lipoplexes by systematic modification of the hydrophobic region of

* Corresponding authors. A.D.M.: tel, +44-(0)-20-7594-5869; fax, +44-(0)-20-7594-5803; e-mail: a.miller@imperial.ac.uk. M.R.J.: tel, +44-(0)-20-7594-3150; fax, +44-(0)-20-7594-1061; e-mail, m.jorgensen@icvec.com.

† Imperial College Genetic Therapies Centre.

‡ Current address: Department of Chemistry, 225, Prospect Street, Yale University, P.O. Box 208107, New Haven, CT 06511-8107.

§ IC-Vec Ltd.

|| Department of Chemistry.

10.1021/jm0507227 CCC: $33.50
Published on Web 11/24/2005

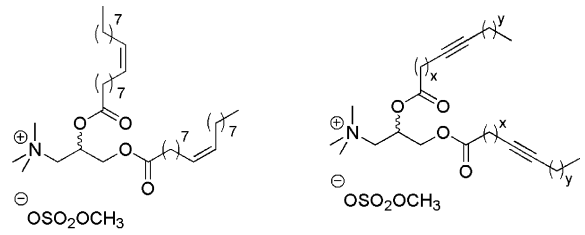

Figure 1. The chemical structures of DOTAP (**1**) and its dialkynoyl analogues (**2**−**4**).

Scheme 1[a]

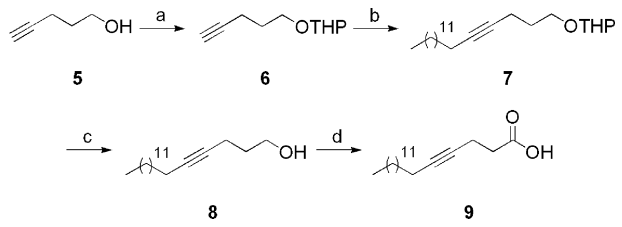

[a] (a) DHP, PPTS, CH_2Cl_2, 0 °C → rt, 15 h, 91%; (b) (i) *n*-BuLi, THF, 0 °C, 15 min; (ii) HMPA, 0 °C, 15 min; (iii) 1-iodotridecane, THF, 0 °C → rt; 20 h, 49%; (d) *p*-TsOH, MeOH, rt, 16 h, 87%; (e) Jones's reagent, 0 °C, 2 h, 67%.

DOTAP lipid tails. A previous group has correlated saturated hydrocarbon chain length for DOTAP with lipoplex stability and biological activity in vitro.[34] Herein we report the modification of the hydrophobic region of the monovalent cationic lipid DOTAP, by substituting the cis-double bonds of the oleate tails with C−C triple bonds, in an effort to alter the membrane properties of the lipoplexes with minimal change to the liposome/micelle−DNA interaction. It was anticipated that fatty acid tails with triple bonds instead of cis-double bonds should exhibit a substantially reduced "kink" and, accordingly, afford more rigid liposomal bilayers. However, these systems should be more fluid than their corresponding fully saturated analogues, such that transfection efficiency is not compromised, as seen elsewhere.[33,34] Lipoplexes (LD particles) containing DOTAP or one of its dialkynoyl analogues were prepared and characterized both physically, using X-ray diffraction and photon correlation spectroscopy, as well as biologically, using reporter gene efficiency assays, both in vitro and in vivo.

Results and Discussion

Chemical Design and Synthesis. The selected modifications made to DOTAP involved both the position and degree of unsaturation of the fatty acyl chains afforded by inserting an acetylenic group at the 4-, 9-, and 14-positions of stearic acid. These changes are shown in Figure 1 as compounds **2**−**4**. The syntheses of the three monoacetylenic analogues of DOTAP first involved the preparation of the monoacetylenic fatty acids. Toward octadec-4-ynoic acid (**9**[35]), THP protection of the hydroxyl group of pent-4-yn-1-ol (**5**), followed by deprotonation of the terminal alkyne with *n*-BuLi and subsequent coupling to 1-iodotridecane (readily furnished from 1-bromotridecane under standard halide exchange conditions) generated the internal alkyne **7**[36] in moderate (49%) yield (Scheme 1). Methanolysis of the THP ether and subsequent Jones's oxidation of the resultant alcohol (**8**[37]) afforded octadec-4-ynoic acid (**9**) as a white powder (26% yield overall). In a similar synthetic route, octadec-9-ynoic acid (**15**[38]) was prepared in five steps from 8-bromooctan-1-ol (**10**) in an overall yield of 38% (Scheme 2).

Scheme 2[a]

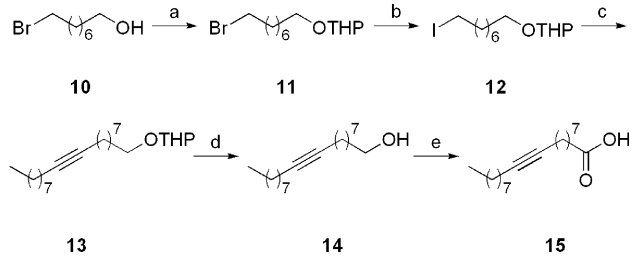

[a] (a) DHP, PPTS, CH_2Cl_2, 0 °C → rt, 16 h, 93%; (b) NaI, $(CH_3)_2CO$, Δ, 15 min, 89%; (c) (i) 1-decyne, *n*-BuLi, THF, 0 °C, 15 min; (ii) HMPA, 0 °C, 15 min; (iii) **12**, THF, 0 °C → rt; 48 h, 72%; (d) *p*-TsOH, MeOH, rt, 20 h, 92%; (e) Jones's reagent, 0 °C, 2 h, 69%.

Scheme 3[a]

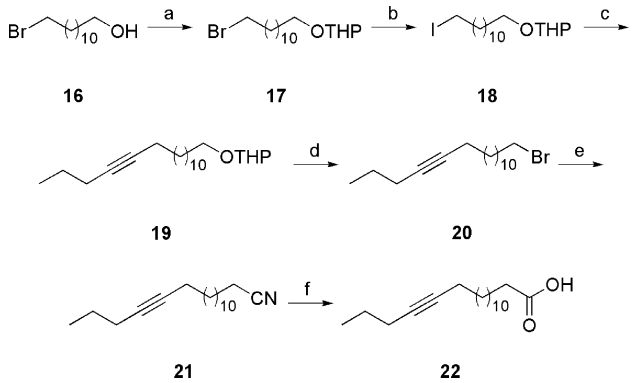

[a] (a) DHP, PPTS, CH_2Cl_2, 0 °C → rt, 16 h, 98%; (b) NaI, $(CH_3)_2CO$, Δ, 20 h, 80%; (c) (i) 1-pentyne, *n*-BuLi, THF, 0 °C, 15 min; (ii) HMPA, 0 °C, 15 min; (iii) **18**, THF, 0 °C → rt; 59%; (d) PPh_3Br_2, PPh_3, CH_2Cl_2, 0 °C, 15 min, 76%; (e) NaCN, DMF, 60 °C, 16 h, 95%; (f) 25 N NaOH, EtOH, Δ, 3 h, 94%.

For the synthesis of octadec-14-ynoic acid (**22**[39]), first the hydroxyl group of 12-bromododecan-1-ol (**16**) was protected quantitatively as its THP ether **17**[40] (Scheme 3). Bromide **17** was converted into the more reactive iodide **18**,[40] with NaI in refluxing acetone, which was then conjugated to 1-pentynyl anion, giving the internal alkyne **19** in moderate yield (59%). Treatment of THP ether **19** with PPh_3Br_2, in the presence of PPh_3 to prevent undesired bromination of the triple bond, furnished the corresponding bromide **20**[36] in a single step and in good yield (76%). Nucleophilic displacement of bromide with cyanide gave nitrile **21**[36] in excellent yield, subsequent basic hydrolysis of which yielded octadec-14-ynoic acid (**22**) as a white powder (94%).

The commercially available, racemic scaffold (±)-3-(dimethylamino)propan-1,2-diol was then fully esterified by coupling to the acid imidazolides of **9**, **15**, and **22**, thereby affording titratable lipids **23** (DS(4-yne)DAP), **24** (DS(9-yne)DAP), and **25** (DS(14-yne)DAP), respectively, in excellent yields (95−98%) (Scheme 4). While the series of dimethylaminopropanyl (DAP) compounds may prove to be interesting pH-dependent cationic lipids in their own right, they were not studied further and converted directly into their corresponding trimethylammoniumpropanyl (TAP) compounds. This was achieved by treating each DAP compound with 6 equivs of dimethyl sulfate in acetone at 4 °C, resulting in the desired quarternary ammonium products (DS(4-yne)TAP (**2**), DS(9-yne)TAP (**3**), and DS(14-yne)TAP (**4**) precipitating rapidly out of solution, as their methyl sulfate salts (75−77%).[41] The yields and purities of the DOTAP analogues are given in Table 1.

Lipoplex Formulation and Physical Characterization. The respective lipids (**1**−**4**) were formulated into liposomes, either

Scheme 4[a]

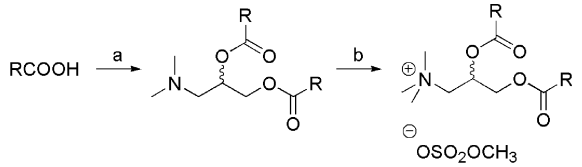

9, **15**, **22** **23 - 25** **2 - 4**

[a] (a) (i) carbonyl diimidazole, $CHCl_3$, rt, 30 min; (ii) (±)-3-(dimethylamino)propan-1,2-diol, DBU, $CHCl_3$, rt, 3 h; (b) Me_2SO_4, $(CH_3)_2CO$, 4 °C, 24 h.

Table 1. Yields for the Synthesis of DODAP Analogues and for Their Conversion to the DOTAP Analogues

acid	DODAP analogue	yield (%)	DOTAP analogue	yield (%), purity (%)[a]
9	**23**	95	**2**	75, >98
15	**24**	98	**3**	76, >98
22	**25**	98	**4**	77, >98

[a] Purity determined by HPLC (see Experimental Section).

Table 2. Liposome and Lipoplex (liposome:DNA (LD) Complexes) Sizes, as Determined by PCS[a]

lipid	liposome (nm)	lipoplex (nm)
DOTAP	89.2 ± 26.0	186.4 ± 77.4
2	98.7 ± 23.4	256.8 ± 55.8
3	73.0 ± 25.5	238.5 ± 60.9
4	40.1 ± 19.1	207.8 ± 66.6
DOTAP:cholesterol (1:1, m/m)	138.8 ± 58.3	223.8 ± 80.4
2:cholesterol (1:1, m/m)	134.6 ± 60.1	246.8 ± 73.2
3:cholesterol (1:1, m/m)	138.2 ± 56.1	187.0 ± 66.7
4:cholesterol (1:1, m/m)	172.4 ± 68.1	230.3 ± 77.1

[a] Standard deviations are given.

on their own or with cholesterol (1:1, m/m), and then complexed with pDNA expressing the β-gal reporter gene to form lipoplexes. The lipid to DNA ratio was kept constant in all cases (10:1, w/w), consistent with the composition of previous DOTAP lipoplexes.[16] Photon correlation spectroscopy (PCS) was used to measure the sizes of all these nanometric particles and results are shown in Table 2. As these data demonstrate, the alteration in the hydrophobic region of the liposomes does not appear to alter their sizes nor the sizes of their related lipoplexes significantly.

X-ray diffraction studies were performed on the lipoplexes and showed that they all adopt the standard lamellar $L_\alpha{}^C$ structure, where DNA rods are intercalated between two lipid bilayers.[42] The largest difference in self-assembled structure from DOTAP lipoplexes was observed with lipoplexes containing analogue **4** (Figure 2). The sharp peaks, labeled q_{001} and q_{002}, give the lamellar repeat distance, $d_{lipid} = 2\pi/q_{001}$. The lipid bilayer repeat distance is d_{lipid} = ca. 60 Å for all analogues. The diffuse, weaker peak, labeled q_{DNA}, results from one-dimensional ordering of the DNA rods within the lipid bilayers and corresponds to a characteristic DNA separation distance of $d_{DNA} = 2\pi/q_{DNA}$. For complexes containing DOTAP, d_{DNA} = 34.0 Å, and this distance increases systematically with the acetylenic analogues as the triple bond is shifted toward the ends of the chains, to d_{DNA} = 40.3 Å for complexes containing analogue **4**. A schematic for the lipoplex structure can be seen in Figure 2C. Since the polar headgroups of the two molecules are identical, these differences in the DNA separation distances, d_{DNA}, may be ascribed to changes in the fatty acyl chain packing.

To understand the variation in the scattering profiles, the thermotropic phase behaviors of the lipids (**1**−**4**) in an aqueous environment were studied using wide-angle X-ray diffraction

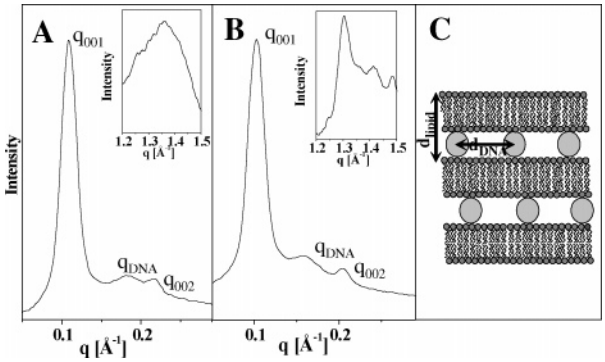

Figure 2. Small-angle X-ray scatterings of lipoplexes show lamellar $L_\alpha{}^C$ structure with variation in the DNA packing between (A) DOTAP and (B) analogue **4**. Wide-angle X-ray scatterings (inset) of liposomes demonstrate (A) fluid-like chain behavior for DOTAP (L_α, broad isotropic peak at q = 1.35 Å^{-1}) and (B) gel-like chain ordering for analogue **4** ($L_{\beta'}$, sharp ordered peak at q = 1.30 Å^{-1}) at 30 °C. (C) Schematic of lamellar lipoplexes with relevant length scales, d_{lipid} and d_{DNA}.[42]

(Figure 2, inset). This serves to simulate the lipid interactions in a liposome assembly. Thus, in this technique the phase transitions of the lipid bilayers can be used to monitor hydrocarbon chain interactions (e.g. van der Waals, steric). This interaction is either represented by a sharp diffraction peak associated with a more rigid, chain-ordered liposome structure ($L_{\beta'}$) or a broad diffraction peak associated with fluid-like structures (L_α).[43,44] The lipid phase transition temperature for the $L_{\beta'}$ to L_α transition was between 20 and 25 °C for DOTAP, similar to that for analogue **2**, but then rose gradually as the triple bond was shifted along the chains, to 30−35 °C for analogue **4**. When liposomes were compared at 30 °C, a chain-melted peak associated with the less stable L_α phase was observed with DOTAP, whereas a chain-ordered peak associated with the $L_{\beta'}$ phase was seen with analogue **4** (Figure 2, inset). These data suggests that relocating the acetylenic bond toward the ends of the fatty acid chains of the lipids confers some level of stability and rigidity to the liposomes and subsequently the lipoplexes. These results are especially pertinent, since near physiological conditions, DOTAP liposomes appear to transform readily into the less stable L_α phase while liposomes containing analogue **4**, in particular, maintain some stable $L_{\beta'}$ phase structure.

Biological Activty: In Vitro. In vitro transfection studies were conducted on HeLa (black), COS-7 (dark gray), and Panc-1 (light gray) cell lines with lipoplexes formed from cationic lipid alone or from cationic lipid:cholesterol liposomes (1:1, m/m) and pDNA containing the luciferase reporter gene (Figure 3). For LD systems prepared from cationic lipid alone, LD transfections of HeLa cells were lowest overall in efficiency, but the transfection efficiencies of lipoplexes prepared with DOTAP-analogue lipids were found to be between 3- and 4-fold higher than the efficiencies of systems prepared with DOTAP. A similar trend was observed with lipoplexes prepared from cationic lipid:cholesterol (1:1, m/m) liposomes. A more dramatic effect was seen with LD transfections of COS-7 and Panc-1 cell lines. For lipoplexes prepared from cationic lipid alone, LD transfections increased only slightly in efficiency when DOTAP was exchanged for analogues **2** or **3** but by a statistically significant 8-fold in COS-7 cells ($p < 0.0001$) and 40-fold in Panc-1 cells ($p = 0.0223$) when analogue **4** was used in place of DOTAP. A similar trend, although not as pronounced, was observed with lipoplexes prepared from cationic lipid:cholesterol (1:1, m/m) liposomes.

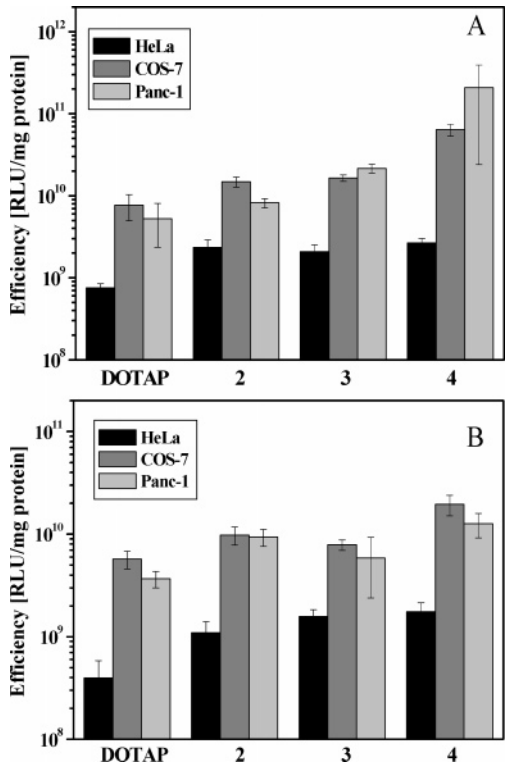

Figure 3. Transfection efficiency (TE) in vitro for LD systems containing DOTAP or analogues (**2**−**4**) and pEGFP-LUC plasmid DNA. TE was assessed for both (A) cationic lipid or (B) cationic lipid:cholesterol (1:1, m/m) formulations on HeLa, COS-7, and Panc-1 cell lines.

This demonstrates that not only does the replacement of the double bond with a triple bond in the acyl chains of DOTAP play a structural role in liposomes and lipoplexes (LD particles) but also a functional role in determining the efficiency of LD transfections. In fact, a comparison may be drawn between the stability imparted by the positional change and the transfection efficiency. As the triple bond is relocated toward the ends of the fatty acid chains, the lipoplex stability at near physiological temperatures appears to increase in line with the associated transfection efficiency, suggesting that, in this case, improved transfection efficiency in vitro may be a function of improved LD particle stability.

To determine whether the observed increase in transfection efficiency results from extracellular events or from intracellular interactions, an uptake assay was performed on Panc-1 cells using lipoplexes prepared from cationic lipid:cholesterol (1:1, m/m) liposomes containing [^{14}C]cholesterol. Panc-1 cells were used since this cell line had shown the most dramatic variance in transfection results for the respective lipoplexes (Figure 4). The uptake profiles of lipoplexes containing either DOTAP or analogues (**2**−**4**) were all similar. After 4 h of transfection, approximately 10% of the LD particles (around 0.05 μg of DNA) were taken up by the cells in all cases. Therefore, intracellular events, such as endosomal release or intracellular trafficking, appear to be dictating the difference observed between transfection efficiencies in vitro.

To ensure that the differences in transfection efficiency in vitro were not due to varying toxicity effects related to DOTAP or analogues (**2**−**4**), a standard cell proliferation assay (MTT, Roche) was performed to show cell viability post-transfection (Figure 5). After transfection, the cells were approximately 70% viable, in comparison to cells not exposed to transfection. The notable aspect here is that approximately the same percentage

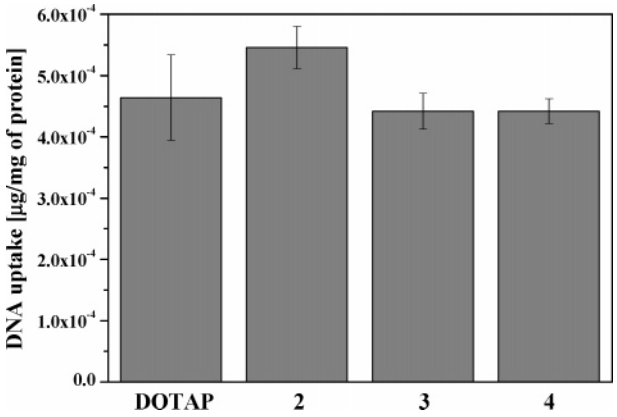

Figure 4. Lipoplex uptake studies performed on Panc-1 cells post-transfection indicate similar uptake profiles for DOTAP and analogues (**2**−**4**) used in this study.

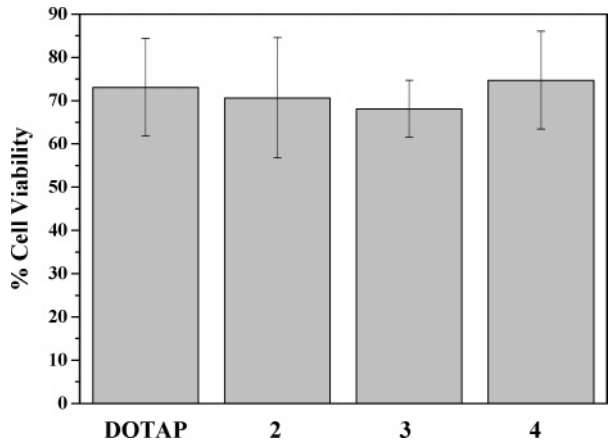

Figure 5. Cell viability studies performed on Panc-1 cells post-transfection indicate similar levels of cell viability for DOTAP and analogues (**2**−**4**) used in this study.

was seen irrespective of lipid type, including DOTAP. This indicates that the cationic headgroup, which is common for all of the lipids, may be responsible for any observed cellular toxicity, and that the alteration of the lipidic tails has little influence on toxicity.

Biological Activity: In Vivo. The real potential of DOTAP lipoplexes is in their ability to mediate transfection in vivo in the lung. This has important implications for the treatment of lung cancer, and a phase I clinical trial is already reported to be recruiting in this regard.[45] To assess the biological relevance of the in vitro findings in an in vivo model, LD systems formulated from cationic lipid:cholesterol (1:1, m/m) cationic liposomes were administered through tail vein injection into Balb-c mice. Transfection efficiency was determined from the level of β-gal protein activity post-delivery of pDNA expressing the β-gal gene (50 μg per mouse) (Figure 6). The efficiencies of LD transfections in vivo of systems formulated with either DOTAP, analogue **2**, or analogue **3** were all very similar. However, with analogue **4**, LD transfection efficiency was increased 2-fold. A two-tailed *t*-test showed this difference to be statistically significant ($p = 0.032$).

This trend was further investigated by comparing lipoplex transfections in vivo with systems formulated using DOTAP or analogue **4** but with alteration of the dose of pDNA delivered to the mice from 25 to 150 μg in several steps (Figure 7). At the lower doses of 25 and 50 μg, lipoplex transfections of systems containing analogue **4** were 2-fold more efficient, in line with previous data (Figure 6). Inflammation was also noted

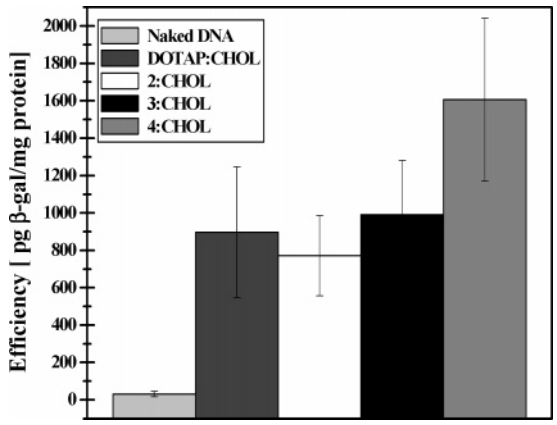

Figure 6. Transfection efficiency in vivo for LD systems formulated from cationic lipid:cholesterol (CHOL) (1:1, m/m) cationic liposomes, containing 50 μg of pUMVC-nt-β-gal pDNA with a fixed lipid:DNA ratio (10:1, w/w). Experiments were conducted using Balb-c mice. Each experiment was repeated six times with the standard deviation denoted by the error bars. Naked DNA is shown as a control.

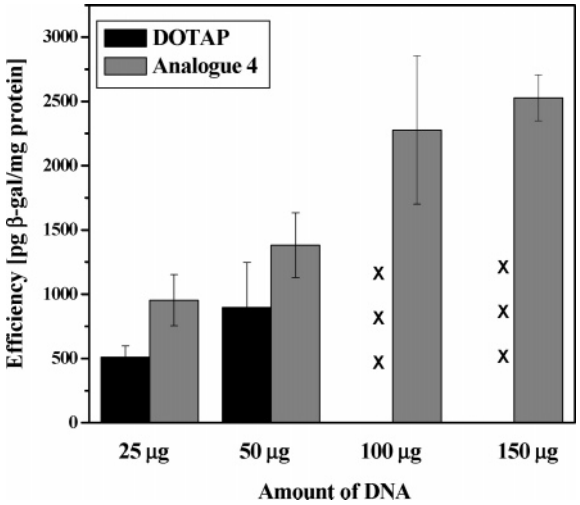

Figure 7. Transfection efficiency in vivo for LD systems formulated from cationic lipid:cholesterol (1:1, m/m) cationic liposomes, containing 25−150 μg of pUMVC-nt-β-gal pDNA with a fixed lipid:DNA ratio (10:1. w/w). Experiments were conducted on Balb-c mice. Each experiment was repeated three times with the standard deviation denoted by the error bars. The data at the higher DNA doses for DOTAP-containing LD systems were omitted (indicated with x) as the animals did not survive to experimental end point.

in lung biopsies of mice administered with lipoplexes formulated from DOTAP. Importantly, when mice were administered higher DNA doses of 100 and 150 μg, lipoplex systems formulated with DOTAP proved fatal, while systems formulated with analogue **4** did not, and animals remained healthy in appearance, although lung biopsies indicated the presence of some inflammation. Nevertheless, this reduced toxicity of the analogue **4**-based vector allowed for an almost 3-fold increase in transgene expression. Similar toxicity behavior has been noted previously in studies by Huang et al., which revealed that DOTAP lipoplexes containing 100 μg of DNA generally caused severe toxicity and sometimes animal death when administered in vivo.[16,21] Several other studies have shown that DOTAP lipoplexes promote the production of proinflammatory cytokines in a dose-dependent fashion. Interestingly, DOTAP liposomes and plasmid DNA administered on their own do not produce such effects and the inflammatory response is due to the lipoplex itself or lipoplex-associated features.[18,22] Such inflammation may be due to intracellular responses to nonmethylated CpG sequences found in the pDNA, and some researchers have shown that higher gene expression in the lung induces hepatoxicity due to an increase in serum transaminase levels.[22] Ramesh and co-workers are making use of small molecule inhibitors directed against inflammation signaling molecules to increase the therapeutic window.[18] Interestingly, lipoplexes formulated from our new analogues, particularly analogue **4** lipoplexes, appear able to mediate higher levels of expression in the lung than the corresponding DOTAP lipoplexes with less associated inflammation or apparent toxicity. It is clear that further investigation is required to elucidate the mechanism of uptake and the intracellular behavior of these particles. However, we would suggest that additional lipoplex stability introduced by replacing DOTAP with analogue **4** lipids could be critical for this higher dose effect and improved lipoplex transfection efficiency in vivo (as well as in vitro). In other words, the lipoplex stability at near physiological temperatures appears to increase in line with the associated transfection efficiency in vitro, suggesting that improved transfection efficiency in vivo may be a function of improved lipoplex stability as well.

Conclusions

A series of novel cationic lipids based on DOTAP architecture was synthesized. These DOTAP analogues (**2**−**4**) were altered such that the oleoyl chains were replaced with unsaturated fatty acids of similar, C18 lengths containing a single alkyne bond at the 4-, 9-, and 14-positions. Although liposomes/micelles and lipoplex systems formulated with these analogues displayed varying physical and biological functionality in comparison to liposomes/micelles and lipoplex systems formulated with DOTAP, the most dramatic difference was observed with lipoplex systems formulated with analogue **4**, which showed better lipoplex transfection in vitro in a variety of cell lines. More importantly, analogue **4** lipids showed significantly higher levels of lipoplex transfection of mouse lung in vivo with much less apparent toxicity in comparison to lipoplex transfections involving systems formulated with DOTAP.

The reason for the higher lipoplex transfection ability of lipoplexes containing analogue **4** is not immediately apparent, since in vitro studies showed similar cellular uptake efficiencies for lipoplex particles containing all analogues and similar cellular viabilities post-transfection. These results suggest that the analogue **4** lipid may impart some enhanced endosomal escape properties and/or promote intracellular events that allow for the more efficient intracellular trafficking of the associated pDNA. X-ray diffraction studies indicate that analogue **4** lipids form more stable liposomes and lipoplex systems near physiological temperatures in comparison to DOTAP, perhaps thereby helping to protect the pDNA during intracellular trafficking from DNA endonucleases. At the same time, the lipid transition is on the cusp of physiologically relevant temperatures, hence preventing overstability and excess rigidity that could otherwise hinder desired cell membrane−lipoplex interactions. Hence, we would further suggest that elements of additional liposomal and lipoplex stability introduced by replacing DOTAP, perhaps with analogue **4** lipids may enhance transfection efficiency in vivo as well as in vitro by providing enhanced protection to pDNA from extracellular DNA endonucleases and from the effects of particle aggregation in serum.

Although enhanced lipoplex stability associated with incorporation of analogue **4** lipids may explain the improved levels of transfection efficiency both in vitro and in vivo in comparison to the DOTAP system, further studies are needed to determine the differences in toxicity in vivo. Nonetheless, the potential of

lipoplexes comprising lead analogue **4** lipids to deliver 2−3 times higher DNA doses to lung endothelial cells in vivo holds great promise for the exploitation of these delivery vehicles in the treatment of lung tumors.

Experimental Section

General Chemicals. *N*-[1-(2,3-Dioleoyloxy)propyl]-*N*,*N*,*N*-trimethylammonium methyl sulfate (DOTAP) and DSPE-rhodamine were obtained from Avanti Polar Lipids (Alabaster, AL). CH_2Cl_2 was distilled over P_2O_5, and other solvents were purchased predried as required. Thin-layer chromatography (TLC) was performed on precoated Merck-Kieselgel 60 F_{254} aluminum-backed plates and revealed with acidic ammonium molybdate(IV), potassium manganate(VII), or other agents as appropriate. Flash column chromatography was accomplished on Merck-Kieselgel 60 (230−400 mesh). All other chemicals were of analytical grade or the best grade available and purchased from Sigma-Aldrich. ^1H and ^{13}C NMR spectra were recorded on a Bruker Advance 400, using residual isotopic solvent ($CDCl_3$, $\delta_H = 7.27$ ppm, $\delta_C = 77.0$ ppm; CD_3OD, $\delta_H = 3.84$ ppm, $\delta_C = 49.05$ ppm) as internal reference. Mass spectra were performed using VG-070B, Joel SX-102, or Bruker Esquire 3000 ESI instruments. IR spectra were obtained on a JASCO FT/IR-620 intra-red spectrometer. UV spectroscopy was conducted on a Pharmacia Biotech UItrospec 4000 spectrometer at defined wavelengths. Analytical HPLC was conducted on a Hitachi-LaChrom L-7150 pump system equipped with a Polymer Laboratories PL-ELS 1000 evaporative light scattering detector. HPLC method 1: Vydac C-4 peptide column (4.6 mm × 250 mm): gradient H_2O (0.1% TFA)/MeCN (0.1% TFA)/MeOH, 0 min (100/0/0), 1−15 min (0/100/0), 25 min (0/100/0), 25.1 min (0/0/100), 45 min (0/0/100), 45.1 min (100/0/0), 55 min (100/0/0); flow 1 mL/min. HPLC method 2: Astec Diol column (4.6 mm × 250 mm): solvent mixture A , hexane/2-propanol/glacial acetic acid/triethylamine 101/21/2/0.1 by volume; solvent mixture B, 2-propanol/water/glacial acetic acid/triethylamine 105/17.5/ 2/0.1; gradient 0 min (95% A/5% B), 20 min (0% A/100% B), 23 (95% A/5% B), 45 min (95% A/5% B); flow 1 mL/min.

Liposome Preparation. A uniform lipid film was obtained by mixing lipid stock solutions in chloroform at 5 mg/mL at the desired ratio of lipids followed by slow removal of solvent in vacuo. The film was subsequently suspended with the appropriate amount of high conductivity (18.2 MΩ) water to a final concentration of either 0.5 mg/mL (in vitro studies), 5 mg/mL (in vivo studies), or 10 mg/mL (X-ray diffraction studies) and sonicated to clarity to ensure unilamellar vesicles.

In Vitro Studies. HeLa, Panc-1, and COS-7 cells were cultured in DMEM (Dulbecco's modified Eagle medium, Gibco BRL) supplemented with 1% (v/v) penicillin−streptomycin (Gibco BRL) and 10% (v/v) fetal calf serum (Gibco BRL) at 37 °C in a humidified atmosphere with 10% CO_2.

For efficiency studies, cells were seeded and transfected with an average of 50 000 cells per well in 24-well plates, resulting in a confluency of 70−80%. Liposome (0.5 mg/mL) and pEGFP-LUC DNA (1 mg/mL; BD biosciences) stock solutions were further diluted with DMEM to a final volume of 0.25 mL, and LD systems, containing 0.5 μg of pEGFP-LUC-DNA, were prepared with a lipid:DNA ratio of 10:1 (w/w) and then added to cells. After 4 h of transfection time, cells were rinsed three times with PBS (phosphate-buffered saline, Gibco BRL) and incubated in supplemented DMEM for an additional 24 h to allow expression of the luciferase gene. Results were quantified using the Promega Luciferase Assay System and a Berthold luminometer (Lumat LB 9507). The BCA Protein Assay (Pierce) was used to determine the amount of total cellular protein for normalization.

For cell viability studies, Panc-1 cells were seeded and transfected as described above. After the 24-h incubation time, a cell proliferation kit (MTT; Roche) assay was used to assess the cell viabilities post-transfection.

For liposomal uptake studies, Panc-1 cells were seeded in 48-well plates, with an average of 30 000 cells per well, resulting in cells 50−70% confluent. The transfection procedure was the same as described above, although the liposomal stock solution contained traces of [^{14}C]cholesterol. After the initial 4-h transfection time, cells were washed twice with PBS and once with heparin (100 μL at 5 mg/mL). The cells were then lysed and stored at −20 °C. Lysates were then treated with solvable and hydrogen peroxide to ensure cellular breakdown. Standard scintillation counting techniques were used to assess the radioactivity of the samples and values were normalized to total cellular protein content using a standard BCA assay.

In Vivo Studies. All experiments were carried out on 7-week-old Balb-c female mice (Harlan, Oxon, UK). The mice were injected, under anesthesia (isoflourane), with 200 μL of LD particles formulated from cationic lipid:cholesterol (1:1, m/m) cationic liposomes, and pUMVC-nt-β-gal pDNA ranging in dose from 25 to 150 μg with a fixed lipid:DNA ratio (10:1, w/w). The lungs were collected after 24 h and homogenized in 1 mL of lysis buffer (Roche). The β-gal protein levels were analyzed with a standard ELISA kit (Roche) and normalized to total protein content (Pierce). Each data point represents an average of six mice ± one standard deviation.

Photon Correlation Spectroscopy. Particle sizes of the liposomes and lipoplexes were measured using dynamic light scattering (Coulter N4 plus). The detector was kept at a fixed angle of 90° and correlations were measured over 60 s in triplicate. Liposome concentrations were kept at approximately 0.5 mg/mL to obtain an adequate signal.

X-ray Scattering. Small-Angle X-ray Scattering (SAXS). Complexes for SAXS studies were prepared by mixing liposomes (10 mg/mL) with 0.2 mg of highly polymerized calf thymus DNA (5 mg/mL; Sigma) to a final weight ratio of lipid:DNA = 10. Data were taken on an in-house rotating copper anode source with Osmic multilayer optics and imaged with a MAR image plate detector.

Wide-Angle X-ray Scattering (WAXS). Liposomes for WAXS studies were prepared in excess water conditions (>50%). Temperature increase was done over 30 s and the sample was allowed to equilibrate for 5 min before measurements. Data were taken on an in-house Bede Microsource generator equipped with an integrated focusing capillary optic (XOS) and imaged with a Gemstar HS intensified CCD detector.

Synthesis. The synthesis of octadec-14-ynoic acid (**22**) is given as a representative example for the synthesis of the alkynoic acids; the full syntheses for octadec-4-ynoic (**9**) and octadec-9-ynoic acid (**15**) are given in the Supporting Information.

2-(12-Bromododecyl-1-oxy)tetrahydropyran (17).[40] 12-Bromododecan-1-ol (**16**; 10.9 g, 41.1 mmol) was dissolved in anhydrous CH_2Cl_2 (200 mL) at 0 °C, under Ar. To the stirred solution was added DHP (4.70 cm^3, 51.4 mmol) and PPTS (1.33 g, 15 mol %). After 30 min, the reaction vessel was removed from the ice bath and allowed to stir for 16 h at room temperature. The reaction mixture was neutralized with aqueous $NaHCO_3$ (150 mL), and the organic phase was separated. The aqueous phase was re-extracted with CH_2Cl_2 (2 × 100 mL), and the combined organic layers were washed with water (100 mL) and brine (100 mL), dried (Na_2SO_4), filtered, and concentrated in vacuo. The residue was purified by silica gel flash chromatography (hexane:EtOAc, 13:1) to furnish **17** as a pale-yellow oil (14.1 g, 98%): R_f 0.34 (hexane:EtOAc, 9:1); ^1H NMR (270 MHz, $CDCl_3$) δ_H 1.20−1.44 (16 H, m, 8 CH_2), 1.45−1.60 (6 H, m, 3 CH_2), 1.61−1.89 (4 H, m, 2 CH_2), 3.32−3.41 (1 H, m, CH_2O), 3.39 (2 H, t, $J = 6.8$ Hz, CH_2Br), 3.44−3.52 (1H, m, CH_2O), 3.67−3.76 (1 H, m, CH_2O), 3.82−3.90 (1 H, m, CH_2O), 4.56 (1 H, t, $J = 3.3$ Hz, OCHO); ^{13}C NMR (100 MHz, $CDCl_3$) δ_C 20.1, 25.9, 26.6 (CH_2), 28.6 ($CH_2CH_2CH_2Br$), 29.1, 29.8, 29.9, 29.9, 29.99, 29.99, 30.1 (7 CH_2), 31.2 (CH_2CHO), 34.3 (CH_2Br), 62.7, 68.0 (2 CH_2O), 99.4 (OCHO); *m*/*z* (FAB^+) 351 ($[M + H]^+$, 5) 349 ($[M + H]^+$, 8), 85 (100), 69 (22), 57 (22), 55 (29); HRMS (FAB^+) calcd for $C_{17}H_{34}O_2{}^{81}Br$ $[M + H]^+$ 351.172171, found 351.174248.

2-(12-Iododododecyl-1-oxy)tetrahydropyran (18).[40] NaI (7.29 g, 48.6 mmol) was dissolved in a stirred solution of **17** (8.50 g, 24.3 mmol) in acetone (250 mL) at room temperature. The reaction system was flushed with N_2 and left under reflux for 20 h. The

white precipitate was filtered off, and the reaction mixture was concentrated in vacuo. The resultant residue was dissolved in CH_2Cl_2 (150 mL) and washed with water (100 mL). The organic layer was separated, and the aqueous layer was extracted further with CH_2Cl_2 (2 × 150 mL). The combined organic layers were washed with water (100 mL) and brine (100 mL), dried ($MgSO_4$), and concentrated in vacuo. The residue was subjected to silica gel flash column chromatography (hexane:EtOAc, 13:1) to afford the title compound (**18**) as a pale-yellow oil (7.75 g, 80%): R_f 0.34 (hexane:EtOAc, 9:1); ^{1}H NMR (270 MHz, $CDCl_3$) δ_H 1.20−1.43 (16 H, m, 8 CH_2), 1.45−1.63 (6 H, m, 3 CH_2), 1.64−1.88 (4 H, m, 2 CH_2), 3.17 (2 H, t, J = 7.0 Hz, CH_2I), 3.32−3.40 (1 H, m, CH_2O), 3.45−3.52 (1 H, m, CH_2O), 3.67−3.76 (1 H, m, CH_2O), 3.81−3.90 (1 H, m, CH_2O), 4.56 (1 H, t, J = 3.5 Hz, OCHO); ^{13}C NMR (100 MHz, $CDCl_3$) δ_C 7.66 (CH_2I), 20.1, 25.9, 26.6, 28.9, 29.8, 29.9, 29.9, 29.9, 29.9, 30.1 (10 CH_2), 30.9 ($CH_2CH_2CH_2I$), 31.2 (CH_2CHO), 34.0 (CH_2CH_2I), 62.7, 68.0 (CH_2O), 99.2 (OCHO); *m*/*z* (FAB^+) 397 ($[M + H]^+$, 6), 395 ($[M - H]^+$, 4), 85 (100), 69 (30), 67 (19), 57 (28), 55 (39); HRMS (FAB^+) calcd for $C_{17}H_{34}O_2I$ $[M + H]^+$ 397.160358, found 397.160049.

2-(Heptadec-13-ynyl-1-oxy)tetrahydropyran (19). To a stirred solution of 1-pentyne (2.25 mL, 22.9 mmol) in anhydrous THF (40 mL) at 0 °C, under a N_2 atmosphere, was added *n*-BuLi (1.80 M in hexanes; 14.3 mL, 25.7 mmol) dropwise. After 15 min, HMPA (40 mL) was added to the bright yellow solution, turning the reaction mixture caramel in color. After a further 15 min, **18** (7.55 g, 19.0 mmol) was added with anhydrous THF (20 mL), turning the solution yellow-orange through blue-green. Within 1.5 h, the solution had turned darker in color. The reaction mixture was allowed to stir at room temperature for a further 48 h and then poured onto an ice/water mixture (200 mL). Crude **19** was extracted with diethyl ether (3 × 200 mL), and the combined organic layers were combined, washed with water (100 mL) and brine (100 mL), dried (Na_2SO_4), and concentrated. The crude residue was purified by flash column chromatography of the residue (hexane:EtOAc, 20:1) to yield **19** as a pale-yellow oil (3.76 g, 59%): R_f 0.19 (hexane:EtOAc, 30:1); ^{1}H NMR (270 MHz, $CDCl_3$) δ_H 0.95 (3 H, t, J = 7.3 Hz, CH_3), 1.21−1.40 (16 H, m, 8 CH_2), 1.41−1.64 (10 H, m, 5 CH_2), 1.65−1.89 (2 H, 2 m, CH_2), 2.06−2.16 (4 H, m, $CH_2C{\equiv}CCH_2$), 3.32−3.41 (1 H, m, CH_2O), 3.44−3.52 (1 H, m, CH_2O), 3.67−3.76 (1 H, m, CH_2O), 3.82−3.90 (1 H, m, CH_2O), 4.56 (1 H, t, J = 3.6 Hz, OCHO); ^{13}C NMR (100 MHz, $CDCl_3$) δ_C 13.2 (CH_3), 18.0, 19.2, 20.01, 22.8, 25.9, 26.7, 29.2, 29.5, 29.9, 29.9, 30.0, 30.1 (15 CH_2), 31.2 (CH_2CHO), 62.6, 68.1 (2 CH_2O), 80.0, 80.3 (C≡C), 99.2 (OCHO); *m*/*z* (FAB^+) 337 ($[M + H]^+$, 4), 335 (3), 238 (4), 85 (100), 81 (10), 69 (9), 67 (11), 57 (8), 55 (15); HRMS (FAB^+) calcd for $C_{22}H_{39}O_2$ $[M - H]^+$ 335.295006, found 335.295944.

1-Bromoheptadec-13-yne (20).[36] To a stirred solution of PPh_3Br_2 (5.87 g, 13.9 mmol) and PPh_3 (1.41 g, 5.36 mmol) in anhydrous CH_2Cl_2 (150 mL) at 0 °C under N_2 was added **19** (3.61 g, 10.7 mmol). After 15 min, excess PPh_3Br_2 was destroyed with 10% aqueous K_2CO_3 solution. The organic phase was separated, and the aqueous phase was re-extracted with CH_2Cl_2 (3 × 150 mL). The combined organic layers were washed with water (150 mL) and brine (150 mL), dried ($MgSO_4$), filtered, and concentrated. Crude **9** was subjected to silica gel column chromatography (100% hexane → 95% hexane:EtOAc → 90% hexane:EtOAc) to furnish the title compound as an 84% pure pale-yellow oil (3.02 g, 90%): R_f 0.61 (hexane:EtOAc, 9:2); ν_{max} (Nujol mull)/cm^{-1} 2199; ^{1}H NMR (300 MHz, $CDCl_3$) δ_H 0.99 (3 H, t, J = 7.4 Hz, CH_3), 1.24−1.58 (18 H, 2 m, 9 CH_2), 1.50 (2 H, sex., J = 7.1 Hz, CH_2CH_3), 1.87 (2 H, quin, J = 7.2 Hz, CH_2CH_2Br), 2.11−2.21 (4 H, m, $CH_2C{\equiv}CCH_2$), 3.43 (2 H, t, J = 6.9 Hz, CH_2Br); ^{13}C NMR (100 MHz, $CDCl_3$) δ_C 13.4 (CH_3), 18.7, 20.9, 22.6, 25.0 ($CH_3CH_2CH_2C{\equiv}CCH_2$, CH_2), 28.6, 29.2, 29.3, 29.6, 29.9, 29.9, 30.0, 30.2 (8 CH_2), 33.2 (CH_2CH_2Br), 34.2 (CH_2Br), 80.0, 80.4 (C≡C); *m*/*z* (EI) 316 (M^+, 0.33), 314 (M^+, 0.45), 109 (38), 95 (77), 82 (43), 81 (100), 67 (100), 56 (47), 55 (54), 49 (58), 41 (78).

Octadec-14-ynenitrile (21).[36] NaCN (0.61 g, 12.5 mmol) was dissolved in a stirred solution of **20** (3.02 g, 9.58 mmol) in anhydrous DMF (150 mL), under Ar. The reaction mixture was allowed to stir for 16 h at 60 °C and then poured into water (300 mL). Crude **21** was extracted into benzene (500 mL, then 4 × 100 mL). The combined organic layers were washed with water (100 mL) and brine (100 mL), dried ($MgSO_4$), filtered, and concentrated in vacuo. The residue was purified by silica gel column chromatography (hexane:EtOAc, 9:1) to afford the title nitrile as a pale-yellow oil (1.99 g, 95%): R_f 0.44 (hexane:EtOAc, 3:1); ν_{max} (Nujol mull)/cm^{-1} 2359, 2246; ^{1}H NMR (300 MHz, $CDCl_3$) δ_H 0.98 (3 H, t, J = 7.4 Hz, CH_3), 1.24−1.58 (18 H, m, 9 CH_2), 1.49 (2 H, sex., J = 7.1 Hz, CH_2CH_3), 1.67 (2 H, quin, J = 7.3 Hz, $CH_2CH_2CH_3$), 2.10−2.21 (4 H, m, $CH_2C{\equiv}CCH_2$), 2.35 (2 H, t, J = 7.1 Hz, CH_2CN); ^{13}C NMR (100 MHz, $CDCl_3$) δ_C 12.5 (CH_3), 16.1, 17.8, 19.8, 21.6, 24.4 ($CH_3CH_2CH_2C{\equiv}CCH_2$, CH_2CH_2CN), 27.7, 27.8, 27.8, 28.2, 28.2, 28.3, 28.5, 28.51, 28.5 (9 CH_2), 79.0, 79.3 (C≡C), 118.8 (CN); *m*/*z* (FAB^+) 262 ($[M + H]^+$, 100), 95 (30), 81 (43), 77 (33), 67 (39), 55 (55), 41 (40); HRMS (FAB^+) calcd for $C_{18}H_{32}N$ $[M + H]^+$ 262.253475, found 262.254333.

Octadec-14-ynoic Acid (22).[39] To a stirred solution of nitrile **21** (1.83 g, 7.00 mmol) in ethanol (2 mL) was added 25 N NaOH solution (1 mL). The reaction mixture was stirred under reflux until no further evolution of ammonia gas could be detected (3 h), poured onto an ice−water mixture (200 mL), and acidified to pH 2 with concentrated aqueous HCl. The crude title acid was extracted into diethyl ether (3 × 200 mL), and the combined organic layers were washed with water (100 mL) and brine (100 mL), dried ($MgSO_4$), filtered, and concentrated, affording **22** in > 95% purity. Crystallization from hexane gave pure **22** as a white powder (1.85 g, 94%): R_f 0.38 (hexane:EtOAc, 2:1); ν_{max} (Nujol mull)/cm^{-1} 2273, 1706; ^{1}H NMR (270 MHz, $CDCl_3$) δ_H 0.95 (3 H, t, J = 7.3 Hz, CH_3), 1.17−1.55 (18 H, 2 m, 9 CH_2), 1.47 (2 H, sex., J = 7.2 Hz, CH_2CH_3), 1.61 (2 H, quin, J = 7.0 Hz, $CH_2CH_2CO_2H$), 2.06−2.20 (4 H, m, $CH_2C{\equiv}CCH_2$), 2.33 (2 H, t, J = 7.4 Hz, CH_2CO_2H); ^{13}C NMR (67.5 MHz, $CDCl_3$) δ_C 13.5 (CH_2), 18.8, 20.8, 22.6, 24.7 ($CH_3CH_2CH_2C{\equiv}CCH_2$, $CH_2CH_2CO_2H$), 28.9, 29.1, 29.2, 29.3, 29.5, 29.6 (9 CH_2), 34.2 (CH_2CO_2H), 80.0, 80.4 (C≡C), 180.7 (CO_2H); *m*/*z* (CI) 298 ($[M + NH_4]^+$, 100), 297 (48), 242 (19), 83 (14), 81 (23), 58 (13); HRMS (CI) calcd for $C_{18}H_{36}NO_2$ $[M + NH_4]^+$ 298.274605, found 298.275163.

General Procedure for Preparation of Tertiary Amino "DAP" Lipids (23, 24, or 25). To a stirred solution of the fatty acid (**9**, **15**, or **22**; 2.67 equiv) in anhydrous $CHCl_3$ (0.2 M) at room temperature and under N_2 was added CDI (3.33 equiv) in one portion. After 30 min, a solution of 3-(dimethylamino)propan-1,2-diol (1 equiv) and DBU (2.67 equiv) in anhydrous $CHCl_3$ (0.5 M, with respect to diol) was added dropwise to the reaction mixture. After 3 h, the mixture was diluted 3-fold with CH_2Cl_2 and then washed with a 0.1 M aqueous solution of KOH (3×). The combined aqueous washes were back-extracted with further CH_2Cl_2 (4×) and then all organic fractions were combined, concentrated, and purified by silica gel column chromatography (hexane:EtOAc, 1:1, with 1% Et_3N) to give the desired DAP compounds as colorless oils that partially crystallized on standing.

1,2-Bis(octadec-4-ynoyloxy)-3-(dimethylamino)propane (DS-(4-yne)DAP, 23): 409 mg (95%); R_f 0.38 (EtOAc); ^{1}H NMR (270 MHz, $CDCl_3$) δ_H 0.86 (6 H, t, J = 6.6 Hz, 2 CH_2CH_3), 1.18−1.36 (40 H, m, 20 CH_2), 1.37−1.49 (4 H, m, 2 $CH_2(CH_2)_{10}CH_3$), 2.05−2.14 (4 H, m, 2 $CH_2(CH_2)_{11}CH_3$), 2.24 (6 H, s, $N(CH_3)_2$), 2.41−2.55 (10 H, m, 2 $CH_2CH_2CO_2$, C3-$H_{a,b}$), 4.06−4.13 (1 H, dd, ^2J = 11.9 Hz, ^3J = 6.4 Hz, C1-H_b), 4.34−4.40 (1 H, dd, ^2J = 11.9 Hz, ^3J = 3.2 Hz, C1-H_a), 5.13−5.23 (1 H, m, C2-H); ^{13}C NMR (400 MHz, $CDCl_3$) δ_C 14.5 (2 CH_2CH_3), 15.1, 15.1, 19.1, 23.1, 29.3, 29.4, 29.6, 29.8, 30.0, 30.1, 30.1, 30.1, 32.3 (26 CH_2), 34.4, 34.6 (2 CH_2CO_2), 46.4 ($N(CH_3)_2$), 59.6 ($CH_2N(CH_3)_2$), 64.5 ($CH_2CHCH_2N(CH_3)_2$), 70.0 ($CHCH_2N(CH_3)_2$), 81.6, 81.6 (2 C≡C), 172.0, 172.2 (2 CO); *m*/*z* (FAB^+) 645 ($[M + H]^+$, 30, 644 (M^+, 60), 84 ($[(CH_3)_2NCH_2C{\equiv}CH + H]^+$, 45), 58 ($[(CH_3)_2N{=}CH_2]^+$, 100); HRMS ($FAB^+$) calcd for $C_{41}H_{73}N_1O_4$, $[M + H]^+$, 644.561786, found 644.561249.

1,2-Bis(octadec-9-ynoyloxy)-3-(dimethylamino)propane (DS-(9-yne)DAP, 24): 423 mg (98%); R_f 0.40 (ethyl acetate); ^{1}H NMR

(400 MHz, $CDCl_3$) δ_H 0.88 (6 H, t, $J = 6.8$ Hz, 2 CH_2CH_3), 1.23−1.66 (48 H, m, 24 CH_2), 2.10−2.16 (8 H, m, 2 $CH_2C{\equiv}CCH_2$), 2.26 (6 H, s, $N(CH_3)_2$), 2.28−2.32 (4 H, m, 2 CH_2CO_2), 2.44 (2 H, m, C3-$H_{a,b}$), 4.08 (1 H, dd, $^2J = 11.6$ Hz, $^3J = 6.4$ Hz, C1-H_b), 4.36 (1 H, dd, $^2J = 11.8$ Hz, $^3J = 3.0$ Hz, C1-H_a), 5.19 (1 H, m, C2-H); ^{13}C NMR (400 MHz, $CDCl_3$) δ_C 14.5 (2 CH_2CH_3), 19.1, 19.1, 23.0, 25.3, 29.0, 29.2, 29.3, 29.3, 29.4, 29.5, 29.5, 29.5, 29.6, 32.2 (26 CH_2), 34.3, 34.5 (2 CH_2CO_2), 46.4 ($N(CH_3)_2$), 59.8 ($CH_2N(CH_3)_2$), 64.2 ($CH_2CHCH_2N(CH_3)_2$), 69.6 ($CHCH_2N(CH_3)_2$), 80.4, 80.7 (2 C≡C), 173.5, 173.8 (2 CO); *m/z* (FAB^+) 645 ($[M + H]^+$, 30), 644 (M^+, 70), 84 ($[(CH_3)_2NCH_2C{\equiv}CH + H]^+$, 42), 58 ($[(CH_3)_2N{=}CH_2]^+$, 100); HRMS ($FAB^+$) calcd for $C_{41}H_{73}N_1O_4$ $[M + H]^+$ 644.561786, found 644.561218.

1,2-Bis(octadec-14-ynoyloxy)-3-(dimethylamino)propane (DS-(14-yne)DAP, 25): 424 mg (98%); R_f 0.37 (ethyl acetate); ^{1}H NMR (270 MHz, $CDCl_3$) δ_H 0.90 (6 H, t, $J = 7.4$ Hz, 2 CH_2CH_3), 1.17−1.34 (34 H, 2 m, 17 CH_2), 1.36−1.48 (6 H, m, 2 CH_2CH_3, CH_2), 1.48−1.58 (4 H, m, $CH_2CH_2CO_2$), 2.02−2.10 (8 H, m, 2 $CH_2C{\equiv}CCH_2$), 2.19 (6 H, s, $N(CH_3)_2$), 2.21−2.26 (4 H, m, 2 CH_2CO_2), 2.32−2.43 (2 H, m, C3-$H_{a,b}$), 3.99−4.04 (1 H, dd, $^2J = 11.9$ Hz, $^3J = 6.4$ Hz, C1-H_b), 4.27−4.32 (1 H, dd, $^2J = 11.9$ Hz, $^3J = 3.1$ Hz, C1-H_a), 5.09−5.17 (1 H, m, C2-H); ^{13}C NMR (400 MHz, $CDCl_3$) δ_C 13.9 (2 CH_2CH_3), 19.1, 21.1, 22.9, 25.3, 25.3, 29.2, 29.5, 29.6, 29.7, 29.9, 29.9, 30.0, 30.0, (26 CH_2), 34.5, 34.8, (2 CH_2CO_2), 46.4 ($N(CH_3)_2$), 59.8 ($CH_2N(CH_3)_2$), 64.2 ($CH_2CHCH_2N(CH_3)_2$), 69.6 ($CHCH_2N(CH_3)_2$), 80.4, 80.7 (2 C≡C) 173.9, 173.6 (2 CO); *m/z* (FAB^+) 645 ($[M + H]^+$, 29), 644 (M^+, 68), 84 ($[(CH_3)_2NCH_2C{\equiv}CH + H]^+$, 37), 58 ($[(CH_3)_2N{=}CH_2]^+$, 100); HRMS ($FAB^+$) calcd for $C_{41}H_{73}N_1O_4$ $[M + H]^+$ 644.561786, found 644.56257.

General Procedure for Preparation of Quarternary Amino "TAP" Lipids as Their Methyl Sulfate Salts (2, 3, and 4). The "DAP" lipids (**23**, **24**, or **25**; 1 equiv) were dissolved in anhydrous acetone (0.1 M) and stirred under N_2 at 0 °C. Then, a solution of dimethyl sulfate (6 equiv) in anhydrous acetone (2 M) was added dropwise. After stirring for 24 h at 4 °C, the reaction mixture was filtered, washing with cold acetone to give the desired "TAP" lipids in approximately 50% yields as white powders. Column chromatography ($CHCl_3$:MeOH:H_2O, 85:13.4:1.6) of the filtrate typically afforded around a further 25% yield of each "TAP" lipid.

***N*-[1-(2,3-(Dioctadec-4-ynoyloxy))propyl]-*N*,*N*,*N*-trimethylammonium methyl sulfate (DS(4-yne)TAP, 2):** 75% (190 mg); R_f 0.39 (CH_2Cl_2:MeOH:H_2O, 65:25:4); ^{1}H NMR (400 MHz, $CDCl_3$) δ_H 0.81 (6 H, t, $^3J = 6.8$ Hz, 2 CH_2CH_3), 1.15−1.30 (40 H, m, 20 CH_2), 1.31−1.43 (4 H, m, 2 $CH_2(CH_2)_{10}CH_3$), 1.98−2.07 (4 H, m, 2 $CH_2(CH_2)_{11}CH_3$), 2.24 (6 H, s, $N(CH_3)_2$), 2.30−2.46 (4 H, m, 2 $CH_2CH_2CO_2$), 2.46−2.55 (4 H, m, 2 $CH_2CH_2CO_2$), 3.34 (9 H, s, $N(CH_3)_3$), 3.63 (3 H, s, CH_3O), 3.72−3.78 (1 H, dd, $^2J = 14.0$ Hz, $^3J = 8.8$ Hz, C3-$H_{a/b}$), 4.06−4.10 (1 H, dd, $^2J = 12.2$ Hz, $^3J = 5.4$ Hz, C1-H_b), 4.22−4.25 (1 H, br d, $^2J = 13.6$ Hz, C3-$H_{b/a}$), 4.45−4.49 (1 H, dd, $^2J = 12.0$ Hz, $^3J = 3.6$ Hz, C1-H_a), 5.51−5.59 (1 H, m, C2-H); ^{13}C NMR (400 MHz, $CDCl_3$) δ_C 14.5 (2 CH_2CH_3), 15.0, 15.0, 19.1, 19.1, 23.1, 29.3, 29.4, 29.4, 29.4, 29.6, 29.8, 30.0, 30.1, 30.1, 30.1, 32.3 (26 CH_2) 34.1, 34.5 (2 CH_2CO_2), 54.6 ($N(CH_3)_3$), 54.8 (CH_3O), 63.7 ($CH_2N(CH_3)_3$), 66.1 ($CH_2CHCH_2N(CH_3)_3$), 66.7 ($CHCH_2N(CH_3)_3$), 81.7, 82.2 (2 C≡C), 171.7, 172.0 (2 CO); *m/z* (FAB^+) 659 ($[M]^+$, 46), 658 ($[M]^+$, 100); HRMS (FAB^+) calcd for $C_{42}H_{76}N_1O_4$ $[M]^+$ 658.577436, found 658.578583; HPLC analysis method 1 $t_R = 29.9$ min (>98% pure), method 2 $t_R = 20.82$ min (>95% pure).

***N*-[1-(2,3-(Dioctadec-9-ynoyloxy))propyl]-*N*,*N*,*N*-trimethylammonium methyl sulfate (DS(9-yne)TAP, 3):** 200 mg (76%); R_f 0.37 (CH_2Cl_2:MeOH:H_2O, 65:25:4); ^{1}H NMR (400 MHz, $CDCl_3$) δ_H 0.81 (6 H, t, $J = 6.7$ Hz, 2 CH_2CH_3), 1.15 − 1.59 (48 H, 2 m, 24 CH_2), 2.04−2.13 (8 H, m, 2 $CH_2C{\equiv}CCH_2$), 2.22−2.32 (4 H, m, 2 CH_2CO_2), 3.29 (9 H, s, $N(CH_3)_3$), 3.63 (3 H, s, CH_3O), 3.63−3.72 (1 H, dd, $^2J = 14.4$ Hz, $^3J = 8.8$ Hz, C3-$H_{a/b}$), 3.98−4.09 (2 H, m, C1-H_b, C3-$H_{b/a}$), 4.41−4.45 (1 H, dd, $^2J = 11.8$ Hz, $^3J = 3.0$ Hz, C1-H_a), 5.52 (1 H, m, C2-H); ^{13}C NMR (400 MHz, $CDCl_3$) δ_C 14.5 (2 CH_2CH_3), 19.1, 19.1, 23.0, 25.0, 25.1, 29.0, 29.1, 29.2, 29.2, 29.3, 29.4, 29.4, 29.5, 29.5, 29.5, 29.6, 32.2 (26 CH_2), 34.2, 34.5 (2 CH_2CO_2), 54.5 ($N(CH_3)_3$), 54.8 (CH_3O), 63.6 ($CH_2N(CH_3)_2$), 66.1 ($CH_2CHCH_2N(CH_3)_3$), 66.3 ($CHCH_2N(CH_3)_3$), 80.4, 80.7 (2 C≡C), 173.1, 173.5 (2 CO); *m/z* (FAB^+) 659 ($[M]^+$, 46), 658 ($[M]^+$, 100); HRMS (FAB^+) calcd for $C_{42}H_{76}N_1O_4$ $[M]^+$ 658.577436, found 658.579575; HPLC analysis method 1 $t_R = 30.6$ min (>98% pure), method 2 $t_R = 21.95$ min (>96% pure).

***N*-[1-(2,3-(Dioctadec-14-ynoyloxy))propyl]-*N*,*N*,*N*-trimethylammonium methyl sulfate (DS(14-yne)TAP, 4):** 77% (205 mg); R_f 0.37 (CH_2Cl_2:MeOH:H_2O, 65:25:4); ^{1}H NMR (400 MHz, $CDCl_3$) δ_H 0.90 (6 H, t, $J = 7.4$ Hz, 2 CH_2CH_3), 1.15−1.34 (32 H, 2 m, 16 CH_2), 1.36−1.48 (8 H, m, 4 CH_2), 1.48−1.58 (4 H, m, 2 $CH_2CH_2CO_2$), 2.02−2.10 (8 H, m, 2 $CH_2C{\equiv}CCH_2$), 2.22−2.30 (4 H, m, 2 CH_2CO_2), 3.32 (9 H, s, $N(CH_3)_3$), 3.63 (3 H, s, CH_3O), 3.66−3.71 (1 H, dd, $^2J = 14.0$ Hz, $^3J = 8.8$ Hz, C3-$H_{a/b}$), 3.99−4.04 (1 H, dd, $^2J = 12.4$ Hz, $^3J = 5.6$ Hz, C1-H_b), 4.11−4.17 (1 H, br d, $^2J = 13.6$ Hz, C3-$H_{b/a}$), 4.41−4.45 (1 H, dd, $^2J = 12.0$ Hz, $^3J = 3.6$ Hz, C1-H_a), 5.49−5.59 (1 H, m, C2-H); ^{13}C NMR (400 MHz, $CDCl_3$) δ_C 13.9 (2 CH_2CH_3), 19.1, 21.2, 22.9, 25.0, 25.1, 29.3, 29.5, 29.5, 29.6, 29.7, 29.7, 29.8, 29.9, 29.9, 30.0, 30.0, 30.0 (26 CH_2), 34.2, 34.6 (2 CH_2CO_2), 54.5 ($N(CH_3)_3$), 54.8 (CH_3O), 63.6 ($CH_2N(CH_3)_2$), 66.2 ($CH_2CHCH_2N(CH_3)_3$), 66.3 ($CHCH_2N(CH_3)_3$), 80.4, 80.8 (2 C≡C), 173.6, 173.2 (2 CO); *m/z* (FAB^+) 659 ($[M + H]^+$, 46), 658 ($[M]^+$, 100); HRMS (FAB^+) calcd for $C_{42}H_{76}N_1O_4$ $[M]^+$ 658.577436, found 658.577713; HPLC analysis method 1 $t_R = 30.7$ min (>98% pure), method 2 $t_R = 22.02$ min (>99% pure).

Acknowledgment. Dr. Steven Fletcher gratefully acknowledges funding from IC-Vec, Ltd. Funding for Dr. Ayesha Ahmad provided by a National Science Foundation, USA, IRFP grant. X-ray diffraction studies were carried out at both the University of California—Santa Barbara (UCSB) facilities by Dr. Cyrus Safinya and Dr. Heather Evans and at Imperial College, London, by Dr. Richard Templer and Andrew Heron.

Supporting Information Available: Table providing results from purity analyses by HPLC, and ^{1}H NMR and ^{13}C NMR spectra for key target compounds (**2** − **4**), and experimental and characterization data for compounds **6**−**9** and **11**−**15**. This material is available free of charge via the Internet at http://pubs.acs.org.

References

(1) Miller, A. D. Cationic liposomes for gene delivery. *Angew. Chem., Int. Ed. Engl.* **1998**, *37*, 1768−1785.
(2) Miller, A. D. The problem with cationic liposome/micelle-based nonviral vector systems for gene therapy. *Curr. Med. Chem.* **2003**, *10*, 1195−1211.
(3) Chesnoy, S.; Huang, L. Structure and function of lipid−DNA complexes for gene delivery. *Annu. Rev. Biophys. Biomol. Struct.* **2000**, *29*, 27−47.
(4) Lasic, D. D.; Templeton, N. S. Liposomes in gene therapy. *Adv. Drug Deliv. Rev.* **1996**, *20*, 221−266.
(5) Brown, M. D.; Schatzlein, A. G.; Uchegbu, I. F. Gene delivery with synthetic (non viral) carriers. *Int. J. Pharm.* **2001**, *229*, 1−21.
(6) Lew, D.; Parker, S. E.; Latimer, T.; Abai, A. M.; Kuwahararundell, A.; et al. Cancer gene-therapy using plasmid DNA—Pharmacokinetic study of DNA following injection in mice. *Hum. Gene Ther.* **1995**, *6*, 553−564.
(7) Mislick, K. A.; Baldeschwieler, J. D. Evidence for the role of proteoglycans in cation-mediated gene transfer. *Proc. Nat. Aca. Sci. U.S.A.* **1996**, *93*, 12349−12354.
(8) Ogris, M.; Brunner, S.; Schuller, S.; Kircheis, R.; Wagner, E. PEGylated DNA/transferrin-PEI complexes: Reduced interaction with blood components, extended circulation in blood and potential for systemic gene delivery. *Gene Ther.* **1999**, *6*, 595−605.
(9) Plank, C.; Mechtler, K.; Szoka, F. C.; Wagner, E. Activation of the complement system by synthetic DNA complexes: A potential barrier for intravenous gene delivery. *Hum. Gene Ther.* **1996**, *7*, 1437−1446.
(10) Kircheis, R.; Schuller, S.; Brunner, S.; Ogris, M.; Heider, K. H.; et al. Polycation-based DNA complexes for tumor-targeted gene delivery in vivo. *J. Gene. Med.* **1999**, *1*, 111−120.
(11) Parker, S. E.; Ducharme, S.; Norman, J.; Wheeler, C. J. Tissue distribution of the cytofectin component of a plasmid−DNA cationic lipid complex following intravenous administration in mice. *Hum. Gene Ther.* **1997**, *8*, 393−401.

(12) Niven, R.; Pearlman, R.; Wedeking, T.; Mackeigan, J.; Noker, P.; et al. Biodistribution of radiolabeled lipid−DNA complexes and DNA in mice. *J. Pharm. Sci.* **1998**, *87*, 1292−1299.
(13) Song, Y. K.; Liu, F.; Chu, S. Y.; Liu, D. X. Characterization of cationic liposome-mediated gene transfer in vivo by intravenous administration. *Hum. Gene Ther.* **1997**, *8*, 1585−1594.
(14) Liu, Y.; Mounkes, L. C.; Liggitt, H. D.; Brown, C. S.; Solodin, I.; et al. Factors influencing the efficiency of cationic liposome-mediated intravenous gene delivery. *Nat. Biotechnol.* **1997**, *15*, 167−173.
(15) Mahato, R. I.; Kawabata, K.; Nomura, T.; Takakura, Y.; Hashida, M. Physicochemical and pharmacokinetic characteristics of plasmid DNA cationic liposome complexes. *J. Pharm. Sci.* **1995**, *84*, 1267−1271.
(16) Li, S.; Rizzo, M. A.; Bhattacharya, S.; Huang, L. Characterization of cationic lipid−protamine−DNA (LPD) complexes for intravenous gene delivery. *Gene Ther.* **1998**, *5*, 930−937.
(17) Ma, Z.; Zhang, J. L.; Alber, S.; Dileo, J.; Negishi, Y.; et al. Lipid-mediated delivery of oligonucleotide to pulmonary endothelium. *Am. J. Respir. Cell Mol. Biol.* **2002**, *27*, 151−159.
(18) Gopalan, B.; Ito, I.; Branch, C. D.; Stephens, C.; Roth, J. A.; et al. Nanoparticle based systemic gene therapy for lung cancer: Molecular mechanisms and strategies to suppress nanoparticle-mediated inflammatory response. *Technol. Cancer Res. Treat.* **2004**, *3*, 647−657.
(19) Ramesh, R.; Saeki, T.; Templeton, N. S.; Ji, L.; Stephens, L. C.; et al. Successful treatment of primary and disseminated human lung cancers by systemic delivery of tumor suppressor genes using an improved liposome vector. *Mol. Ther.* **2001**, *3*, 337−350.
(20) Ramesh, R.; Ito, I.; Saito, Y.; Wu, Z.; Mhashikar, A. M.; et al. Local and systemic inhibition of lung tumor growth after nanoparticle-mediated mda-7/IL-24 gene delivery. *DNA Cell Biol.* **2004**, *23*, 850−857.
(21) Li, S.; Huang, L. In vivo gene transfer via intravenous administration of cationic lipid−protamine−DNA (LPD) complexes. *Gene Ther.* **1997**, *4*, 891−900.
(22) Loisel, S.; Le Gall, C.; Doucet, L.; Ferec, C.; Floch, V. Contribution of plasmid DNA to hepatotoxicity after systemic administration of lipoplexes. *Hum. Gene Ther.* **2001**, *12*, 685−696.
(23) Tousignant, J. D.; Gates, A. L.; Ingram, L. A.; Johnson, C. L.; Nietupski, J. B.; et al. Comprehensive analysis of the acute toxicities induced by systemic administration of cationic lipid: Plasmid DNA complexes in mice. *Hum. Gene Ther.* **2000**, *11*, 2493−2513.
(24) Gautam, A.; Densmore, C. L.; Waldrep, J. C. Pulmonary cytokine responses associated with PEI-DNA aerosol gene therapy. *Gene Ther.* **2001**, *8*, 254−257.
(25) Li, S.; Wu, S. P.; Whitmore, M.; Loeffert, E. J.; Wang, L.; et al. Effect of immune response on gene transfer to the lung via systemic administration of cationic lipidic vectors. *Am. J. Physiol.-Lung Cell. Mol. Physiol.* **1999**, *276*, L796-L804.
(26) Ewert, K.; Ahmad, A.; Evans, H. M.; Schmidt, H. W.; Safinya, C. R. Efficient synthesis and cell-transfection properties of a new multivalent cationic lipid for nonviral gene delivery. *J. Med. Chem.* **2002**, *45*, 5023−5029.
(27) Lasic, D. D. Recent developments in medical applications of liposomes: sterically stabilized liposomes in cancer therapy and gene delivery in vivo. *J. Controlled Release* **1997**, *48*, 203−222.
(28) Byk, G.; Dubertret, C.; Escriou, V.; Frederic, M.; Jaslin, G.; et al. Synthesis, activity, and structure−activity relationship studies of novel cationic lipids for DNA transfer. *J. Med. Chem.* **1998**, *41*, 224−235.
(29) Drummond, D. C.; Zignani, M.; Leroux, J. C. Current status of pH-sensitive liposomes in drug delivery. *Prog. Lipid Res.* **2000**, *39*, 409−460.
(30) Fletcher, S.; Jorgensen, M. R.; Miller, A. D. Facile preparation of an orthogonally protected, pH-sensitive, bioconjugate linker for therapeutic applications. *Org. Lett.* **2004**, *6*, 4245−4248.
(31) Wetzer, B.; Byk, G.; Frederic, M.; Airiau, M.; Blanche, F.; et al. Reducible cationic lipids for gene transfer. *Biochem. J.* **2001**, *356*, 747−756.
(32) Byk, G.; Wetzer, B.; Frederic, M.; Dubertret, C.; Pitard, B.; et al. Reduction-sensitive lipopolyamines as a novel nonviral gene delivery system for modulated release of DNA with improved transgene expression. *J. Med. Chem.* **2000**, *43*, 4377−4387.
(33) Felgner, J. H.; Kumar, R.; Sridhar, C. N.; Wheeler, C. J.; Tsai, Y. J.; et al. Enhanced gene delivery and mechanism studies with a novel series of cationic lipid formulations. *J. Biol. Chem.* **1994**, *269*, 2550−2561.
(34) Regelin, A. E.; Fankhaenel, S.; Gurtesch, L.; Prinz, C.; von Kiedrowski, G.; et al. Biophysical and lipofection studies of DOTAP analogues. *Biochim. Biophys. Acta (BBA)−Biomembr.* **2000**, *1464*, 151−164.
(35) Gunstone, F. D.; Ismail, I. A. Fatty acids. XV. Nuclear magnetic resonance spectra of the cis-octadecenoic acids and of some acetylenic acids. *Chem. Phys. Lipids* **1967**, *1*, 337−340.
(36) Pisch, S.; Bornscheuer, U. T.; Meyer, H. H.; Schmid, R. D. Properties of unusual phospholipids. IV: Chemoenzymic preparation of phospholipids bearing acetylenic fatty acids. *Tetrahedron* **1997**, *53*, 14627−14634.
(37) Valicenti, A. J.; Pusch, F. J.; Holman, R. T. Synthesis of octadecynoic acids and [1-^{14}C] labeled isomers of octadecenoic acids. *Lipids* **1985**, *20*, 234−242.
(38) Berry, D. E.; Chan, J. A.; MacKenzie, L.; Hecht, S. M. 9-Octadecynoic acid: A novel DNA binding agent. *Chem. Res. Toxicol.* **1991**, *4*, 195−198.
(39) Barve, J. A.; Gunstone, F. D. Fatty acids. 33. Synthesis of all the octadecynoic acids and all the *trans*-octadecenoic acids. *Chem. Phys. Lipids* **1971**, *7*, 311−323.
(40) Wasserman, H. H.; Gambale, R. J.; Pulwer, M. J. Activated carboxylates from the photooxygenation of oxazoles. Application to the synthesis of recifeiolide, curvularin, and other macrolides. *Tetrahedron* **1981**, *37*, 4059−4067.
(41) Massing, U.; Kley, J. T.; Gurtesch, L.; Fankhaenel, S. A simple approach to DOTAP and its analogues bearing different fatty acids. *Chem. Phys. Lipids* **2000**, *105*, 189−191.
(42) Rädler, J. O.; Koltover, I.; Salditt, T.; Safinya, C. R. Structure of DNA-cationic liposome complexes: DNA intercalation in multilamellar membranes in distinct interhelical packing regimes. *Science* **1997**, *275*, 810−814.
(43) Cevc, G.; Marsh, D. *Phospholipid Bilayers: Physical Principals and Models*; John Wiley & Sons: New York, 1987.
(44) Winter, R. Synchrotron X-ray and neutron small-angle scattering of lyotropic lipid mesophases, model biomembranes and proteins in solution at high pressure. *Biochim. Biophys. Acta*−Protein Struct. *Mol. Enzymol.* **2002**, *1595*, 160−184.
(45) For information on this trial, see website address www.clinicaltrial.gov and refer to ClinicalTrials.gov Identifier NCT00059605.

JM0507227